Journal of Medicinal Chemistry

pubs.acs.org/jmc

Article

A "Two-Birds-One-Stone" Approach toward the Design of Bifunctional Human Immunodeficiency Virus Type 1 Entry Inhibitors Targeting the CCR5 Coreceptor and gp41 N-Terminal Heptad Repeat Region

Chao Wang,*,‖ Xinling Wang,‖ Huan Wang, Jing Pu, Qing Li, Jiahui Li, Yang Liu,* Lu Lu,* and Shibo Jiang*

Cite This: https://doi.org/10.1021/acs.jmedchem.1c00781

Read Online

ACCESS | Metrics & More | Article Recommendations | Supporting Information

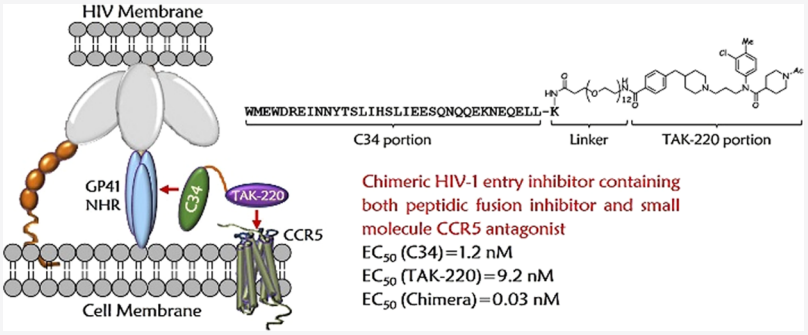

ABSTRACT: Previous studies have reported the stepwise nature of human immunodeficiency virus type 1 (HIV-1) entry and the pivotal role of coreceptor CCR5 and the gp41 N-terminal heptad repeat (NHR) region in this event. With this in mind, we herein report a dual-targeted drug compound featuring bifunctional entry inhibitors, consisting of a piperidine-4-carboxamide-based CCR5 antagonist, TAK-220, and a gp41 NHR-targeting fusion-inhibitory peptide, C34. The resultant chimeras were constructed by linking both pharmacophores with a polyethylene glycol spacer. One chimera, CP12TAK, exhibited exceptionally potent antiviral activity, about 40- and 306-fold over that of its parent inhibitors, C34 and TAK-220, respectively. In addition to R5-tropic viruses, CP12TAK also strongly inhibited infection of X4-tropic HIV-1 strains. These data are promising for the further development of CP12TAK as a new anti-HIV-1 drug. Results show that this strategy could be extended to the design of therapies against infection of other enveloped viruses.

INTRODUCTION

Drug discovery in the treatment of many multifactorial diseases, such as infections, cancers, and degenerative CNS disorders, is gradually moving from the "one molecule−one target−one disease" paradigm to the development of therapeutics able to simultaneously manipulate multiple biological targets to generate satisfactory efficacy.[1,2] Focusing on human immunodeficiency virus type 1 (HIV-1) infection, combinations of two or more antiretroviral medications that act on different aspects of the HIV-1 life cycle, termed combinatorial antiretroviral therapy (cART), fundamentally changed the nature of HIV-1/AIDS treatment.[3,4] The powerful cART approach, which relies on a mixture of monotherapies, has had considerable success in improving drug efficacy and attenuating the development of drug resistance compared with single-target antiviral drug utilities. Still, such drug combination formulations are hindered by possible drug−drug interactions, pharmacokinetic/pharmacodynamic complexity, and cumulative toxicities, collectively motivating the search for novel therapeutic methodologies.[5,6] An alternative to these drug cocktail, or fixed-dose, combinations is a simplified multitarget-directed ligand (MTDL) design strategy. In this approach, a single molecule can interact with multiple proteins, thereby offering higher therapeutic efficiency and delayed drug resistance, while circumventing the pitfalls of combination therapy. As such, MTDLs have gained increasing attention from drug discovery researchers.[1,7,8] Here, we exploit MTDLs for the treatment of HIV-1 infection. With significant progress in elucidating HIV-1 entry into host cells at the molecular

Received: April 29, 2021

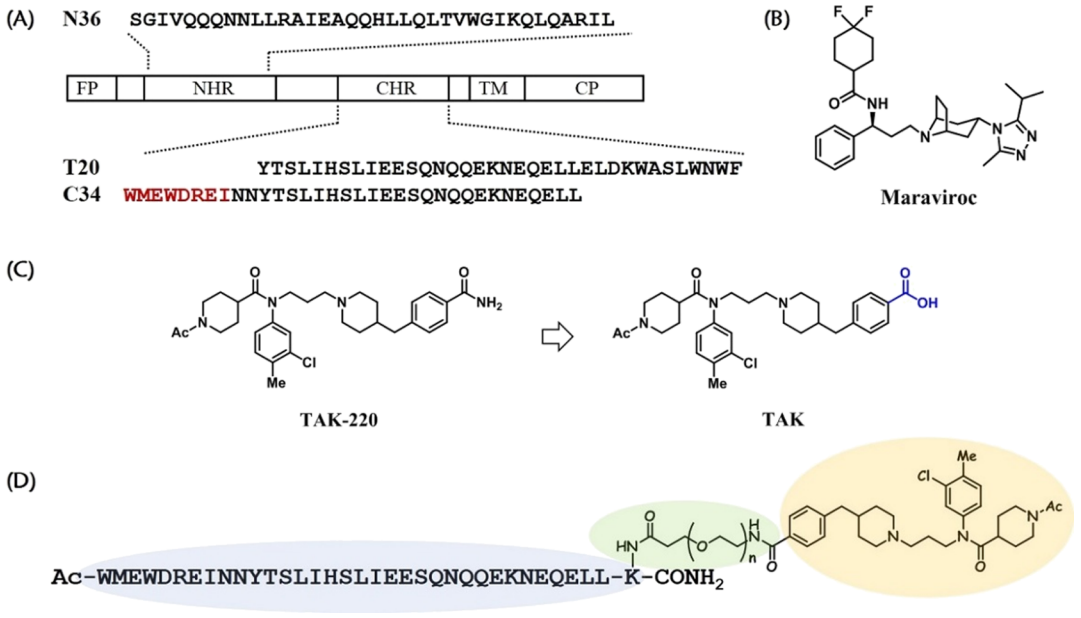

Figure 1. Schematic representation of HIV-1 gp41 and related virus entry inhibitors. (A) HIV-1 gp41 contains different functional domains, including fusion peptide, NHR, CHR, transmembrane domain, and cytoplasm domain. The amino acid sequences of peptide fusion inhibitors T20 and C34, along with their respective target N36, are also shown. The pocket-binding domain (PBD) in C34 peptide is highlighted in red. (B) Structure of small-molecule CCR5 antagonist maraviroc. (C) TAK-220 and its carboxylic acid derivative TAK. (D) Dual-target design strategy. In this study, HIV-1 fusion inhibitor C34 and CCR5 antagonist TAK-220 pharmacophores have been incorporated into the chimera. Suitable PEG spacers of different lengths were used in which n represents the number of PEG units in the linker.

level, events in this highly orchestrated process of HIV-1 invasion were selected as targets for our multitarget inhibitor design.

The accepted mechanism of HIV-1 infection involves initial binding of viral envelope glycoprotein (Env) surface subunit gp120 to the cellular receptor CD4, which, in turn, triggers a series of conformational changes of gp120 that allow it to associate with a chemokine coreceptor, CCR5 or CXCR4, on the target cell.[9,10] Coordinated engagement of CD4 and the chemokine receptor activates the fusion machinery in Env transmembrane subunit gp41. Then, a gp41-central six-helix bundle (6-HB) is subsequently formed through condensation of its N-terminal heptad repeat (NHR) and C-terminal heptad repeat (CHR) regions, providing the critical driving force that facilitates the fusion between the viral envelope and host cell membrane.[11,12]

Inhibition of HIV-1 entry can be achieved by disruption of each of these stages in the early viral life cycle.[9] For example, intensive development of CCR5 antagonists able to disrupt gp120−CD4 coreceptor interaction led to the first marketed CCR5 inhibitor, maraviroc, for treatment-experienced patients.[13,14] However, maraviroc is active only against R5 HIV-1 strains.[15] Consequently, maraviroc therapy failed against preexisting minor CXCR4-tropic X4 HIV-1 strains in the early stage of HIV-1 infection and the incidence of CXCR4-using variants associated with the disease progression.[16] Another approach inhibited the binding of the gp41 CHR to NHR, thus blocking the formation of the fusogenic 6-HB core structure.[9,11,12] During gp41-mediated HIV-1 infection, a fairly long-lived intermediate conformation exists in which NHR helices form a trimeric coiled coil with three hydrophobic grooves that make perfectly susceptible drug targets.[12] More specifically, peptide-based inhibitors are derived from the gp41 CHR region.[17−19] Designated as C-peptides, these inhibitors act by competitively binding to the exposed grooves on NHR-trimer and have been shown to potently curtail HIV-1 activity. One of these C-peptides, enfuvirtide (Fuzeon, T20),[20] received FDA approval in 2003 as the first HIV-1 fusion inhibitor-based anti-HIV drug (Figure 1A,B). However, the low potency and low genetic barrier for drug resistance of T20 have caused a growing number of patients to fail in their response to T20 therapy, thus limiting its clinical use.[21]

Inspired by the multistep nature of the HIV-1 entry process and multiple viable molecular targets involved in this pathway, we herein describe the rational design of MTDLs able to inhibit two crucial stages of HIV-1 cell fusion and entry: the binding of HIV-1 gp120 to its coreceptor CCR5 and gp41 6-HB core formation. The design of such a dual-targeted drug compound features bifunctional entry inhibitors, a CCR5 small-molecule antagonist (TAK-220) and a C-peptide fusion inhibitor (C34) tethered via a poly(ethylene glycol) (PEG) linker. As anticipated, one chimera, CP12TAK, exhibited exceptionally potent antiviral activity, about 40- and 306-fold over that of its parent inhibitors, C34 and TAK-220, respectively. This dual-targeted compound has anti-HIV-1 activity in picomolar concentration against a panel of R5-tropic viral isolates. Unlike its parent CCR5 antagonist TAK-220, it has activity against X4-tropic and dual-tropic viruses. CP12TAK also retained high potency against T20-resistant viruses, conferring cross-resistance to the parental C34 peptide. Our study provides tantalizing insights into developing MTDLs that govern the HIV-1 entry process. Considering the common cascade of events in viral entry,[22,23] our multitarget design strategy in the context of HIV-1 invasion has the potential for application to therapeutic intervention against other enveloped viruses.

DESIGN AND CHEMISTRY

Some key issues in the design of CCR5/gp41 dual-targeted inhibitors include selection of suitable CCR5 antagonists and

https://doi.org/10.1021/acs.jmedchem.1c00781
J. Med. Chem. XXXX, XXX, XXX−XXX

Scheme 1. Synthesis of TAK[a]

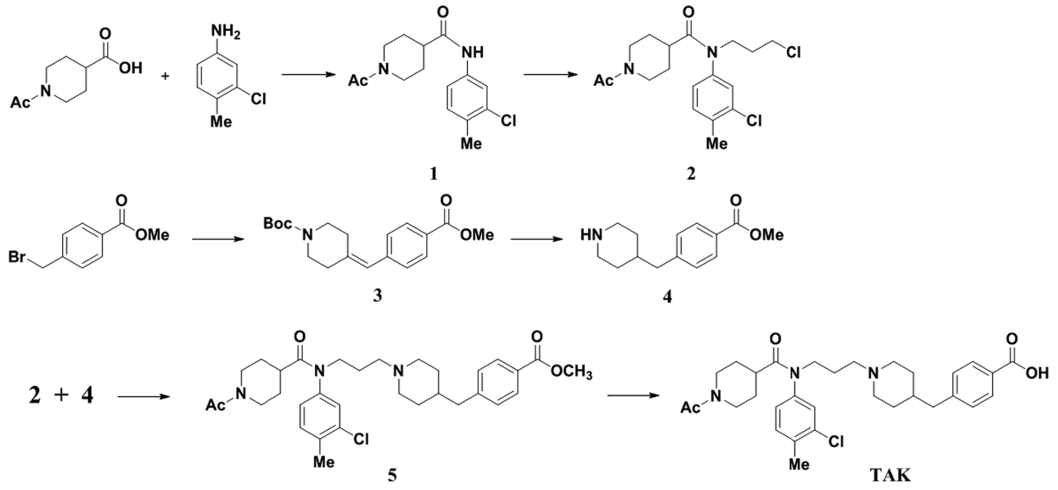

[a]Reagents and conditions: (a) N,N′-carbonyldiimidazole, THF, r.t.; (b) NaH, 1-bromo-3-chloropropane, DMF, 0 °C to r.t.; (c) $(EtO)_3P$; (d) 1-Boc-4-piperidone, NaH, THF; (e) H_2, Pd/C, MeOH; (f) HCl/EtOAc, MeOH; (g) KI, K_2CO_3, DMF/CH_3CN, reflux; (h) 1 M NaOH, dioxane

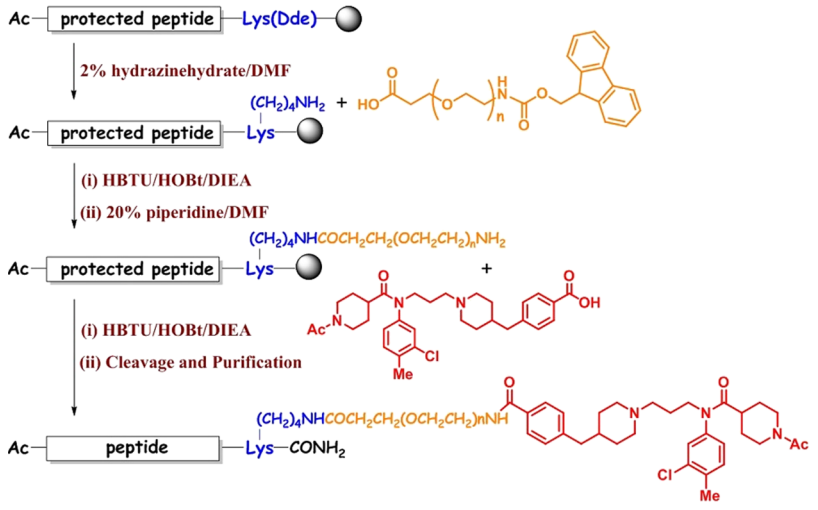

Figure 2. Schematic representation of the strategy used for the preparation of bifunctional molecules.

peptidic fusion inhibitors, identification of proper linkage points of small-molecule CCR5 inhibitors to peptides, and optimization of the length of PEG spacers. In the early 1990s, exploration of peptide fusion inhibitors started with several synthetic peptides overlapping gp41 NHR and CHR regions, including DP-107, SJ-2176, and DP-178 (it was renamed T20 later).[17−19] Two C-peptides, T20 and C34,[11,12] effectively blocked HIV-1 fusion in a low nanomolar range and have been extensively exploited. Interestingly, although T20 was developed as the only membrane fusion inhibitor for clinical use 18 years ago, its mechanism of action has been a matter of debate until recently.[24,25] In contrast, the specific structural properties of C34 in complex with an NHR-derived target mimic peptide, N36, have been finely delineated by crystallographic analysis.[12] C34 has a well-defined mechanism of action and higher HIV-1 inhibitory potency compared with T20. Consequently, C34 is widely used as a design template for the engineering of novel fusion inhibitors.[26] Following this logic, we chose to use C34 as the fusion inhibitor portion of our dual-target scaffold. For the coreceptor part of this hybrid compound, we selected TAK-220, a piperidine-4-carboxamide CCR5 antagonist, first disclosed by Takeda, based on its conformational flexibility and highly potent anti-HIV-1 activity.[27] In selecting a point of attachment for the linker on TAK-220, replacement of the amide group in the right-side phenyl ring with a carboxylic acid moiety was chosen, owing to anticipated low interference with the antiviral potency of TAK-220 after covalent conjugation of the free-acid form of TAK and PEG spacers (Figure 1C).[28] Previous studies suggested the need for antiparallel orientation of C-peptides relative to the viral NHR region and the importance of C-terminal derivatization for their activity pattern.[29−31] Based on the above considerations, TAK was covalently linked to the C-terminus of C34 peptides using flexible PEG linkers with various lengths (hereinafter termed PEGn in which n represents the number of PEG units in the linker) (Figure 1D). A PEG spacer was selected for the multitargeted ligand design because its hydrophilicity would be beneficial to aqueous solubility of the chimeric inhibitors and, hence, avoid any nonspecific hydrophobic contact with either of the target proteins.[32]

The synthetic pathway to TAK is illustrated in Scheme 1. The aniline was coupled with commercially available 1-acetylpiperidine-4-carboxylic acid to afford compound **1**. In

https://doi.org/10.1021/acs.jmedchem.1c00781
J. Med. Chem. XXXX, XXX, XXX−XXX

Table 1. Inhibition of Dual-Target Entry Inhibitors on Laboratory-Adapted HIV-1 R5 Virus Infection[a]

compound	sequence[b]	EC_{50} (nM)
CP0TAK	WMEWDREINNYTSLIHSLIEESQNQQEKNEQELLK(-----TAK)	0.25 ± 0.05
CP4TAK	WMEWDREINNYTSLIHSLIEESQNQQEKNEQELLK(PEG4-TAK)	0.63 ± 0.23
CP8TAK	WMEWDREINNYTSLIHSLIEESQNQQEKNEQELLK(PEG8-TAK)	0.49 ± 0.43
CP12TAK	WMEWDREINNYTSLIHSLIEESQNQQEKNEQELLK(PEG12-TAK)	0.03 ± 0.01
CP24TAK	WMEWDREINNYTSLIHSLIEESQNQQEKNEQELLK(PEG24-TAK)	0.89 ± 0.35
C34	WMEWDREINNYTSLIHSLIEESQNQQEKNEQELL	1.19 ± 0.41
TAK-220		9.18 ± 5.78
C34/TAK-220[c]		0.58 ± 0.16
CP12	WMEWDREINNYTSLIHSLIEESQNQQEKNEQELLK(PEG12-Ac)	3.29 ± 1.73
CP12/TAK-220[c]		2.08 ± 1.69
P26TAK	NNYTSLIHSLIEESQNQQEKNEQELLK(PEG12-TAK)	>50
T20	YTSLIHSLIEESQNQQEKNEQELLELDKWASLWNWF	1.58 ± 0.27

[a]The assay was performed in triplicate, and the data are expressed as the mean ± standard deviation. CEMx174 5.25M7 cells expressing both CCR5 and CXCR4 on the surface were infected with the HIV-1 BaL strain (subtype B, R5). [b]For these peptides, the N-termini were acetylated, and the C-termini were amidated. [c]Molar ratios of C34/TAK-220 or CP12/TAK-220 in combination were 1:1.

the presence of NaH, N-alkylation with 1-bromo-3-chloropropane accessed chloride **2**. Olefin **3** was prepared through the Arbuzov reaction and Horner−Wadsworth−Emmons reaction, using literature procedures[27] and converted into **4** after hydrogenation followed by deprotection of the Boc group. Chlorides were reacted with 4-substituted piperidines in the presence of potassium iodide and potassium carbonate to give compound **5**. By saponification, the methyl ester intermediate **5** was converted into TAK.

We employed an Fmoc solid-phase peptide synthesis protocol to construct a modified version of C34 peptides in which a lysine residue with a 1-(4,4-dimethyl-2,6-dioxocyclohexylidene)ethyl (Dde) side-chain-protecting group was incorporated into the C-terminus of C34 to enable ligation with the carboxyl group of the PEG linkers after selective removal of the Dde group on resin by 2% hydrazinehydrate/ N,N-dimethylformamide (DMF)-mediated deprotection. TAK was then conjugated with PEG spacers, and the corresponding bifunctional molecules were obtained after removal of all peptide protection groups and cleavage of the peptides from resin using TFA (Figure 2).

RESULTS

Dual-Targeted Peptides Effectively Inhibited Infection of Laboratory-Adapted HIV-1 Strains. First, inhibitory activity of dual-targeted peptides on infection by R5 HIV-1 strain BaL (subtype B) on CEMx174 5.25M7 cells was measured. As shown in Table 1, C34, TAK-220, and their 1:1 molar combination exhibited anti-HIV-1 activity with half-maximal effective concentration (EC_{50}) values at 1.2, 9.2, and 0.6 nM, respectively. Chimeric inhibitors without the PEG spacer and with PEG4-, PEG8-, and PEG24-based linkers possessed potency similar to that of the 1:1 mixture of the individual C34 and TAK-220. Strikingly, CP12TAK with 12 PEG units showed high efficacy in inhibiting HIV-1 BaL infection with an EC_{50} value of 0.03 nM, which is 52-fold more potent than that of T20 (EC_{50} = 1.58 nM). Deletion of the N-terminal PBD motif in the C34 portion of CP12TAK, or the CCR5 small-molecule antagonist part of the chimera, resulted in a remarkable decrease of antiviral activity. We further evaluated the antiviral activity of CP12TAK against X4 HIV-1 strain IIIB (subtype B) infection, in comparison with C34, TAK-220, and a mixture of C34 with TAK-220 (1:1 ratio, unlinked). Surprisingly, consistent with the results of laboratory-adapted HIV-1 BaL strain, CP12TAK had an EC_{50} value of 0.03 nM against HIV-1 IIIB on CEMx174 5.25M7 cells that express both CCR5 and CXCR4 receptors, which is approximately 84-fold more potent than that of the 1:1 mixture of C34 with TAK-220 (Table 2). We then assessed

Table 2. Inhibition of CP12TAK on Laboratory-Adapted X4 HIV-1 IIIB Infection[a]

HIV-1 strain (subtype, tropism)	EC_{50} (nM)[b]			
	CP12TAK	C34	TAK-220	C34/TAK-220[c]
IIIB (B, X4)	0.03 ± 0.01	1.62 ± 0.32	>50	2.54 ± 0.85

[a]The assay was performed in triplicate, and the data are expressed as the mean ± standard deviation. [b]CEMx174 5.25M7 cells expressing both CCR5 and CXCR4 on the surface were infected with the HIV-1 IIIB strain (subtype B, X4). [c]The molar ratio of C34/TAK-220 in combination was 1:1.

the potential cytotoxicity of the CP12TAK peptide on target cells used for viral inhibition assays and found that the concentration for 50% cytotoxicity (CC_{50}) was beyond 5000 nM (Figure S1), suggesting that CP12TAK is an effective HIV-1 entry inhibitor with low or no *in vitro* toxic effect.

Potent Antiviral Activity of CP12TAK against Clinical HIV-1 Isolates and T20-Resistant Strains. In addition to the laboratory-adapted HIV-1 BaL and IIIB strains, we also tested the inhibitory activity of CP12TAK against a panel of HIV-1 clinical isolates of subtypes A, B, C, D, F, O, and A/E. As shown in Table 3, CP12TAK exhibited highly potent activity against divergent R5 HIV-1 clinical isolates, including 91US_4, 00TZ_A125, and BCF02, with EC_{50} values of 0.02 to 2.1 nM, which are about 3.5- to 465-fold more potent than that of the 1:1 mixture of C34 and TAK-220. After further testing on X4 HIV-1 clinical isolates, including 92UG024, BZ167/GS010, and MN/H9, CP12TAK was found to be 4.2- to 6.9-fold more potent than that of C34. CP12TAK also had potent inhibitory activity against two R5/X4 dual-tropic isolates. The EC_{50} values were 1.9 and 1.6 nM against 93/BR/020 and 97TH_NP1525, respectively. Furthermore, the inhibitory activity of CP12TAK on the replication of T20-resistant strains was determined. T20 could potently inhibit infection by a T20-sensitive strain with an EC_{50} value of 4.3 nM, but it was much less effective against the T20-resistant strains, including HIV-$1_{NL4\text{-}3(D36G)V38E/N42S}$ (EC_{50} = 261 nM), HIV-

https://doi.org/10.1021/acs.jmedchem.1c00781
J. Med. Chem. XXXX, XXX, XXX−XXX

Table 3. Inhibitory Effect of CP12TAK against Infection by Primary HIV-1 Isolates[a]

HIV-1 isolate	subtype	tropism	EC_{50} (nM)[b]			
			C34	TAK-220	C34/TAK-220	CP12TAK
91US_4	B	R5	74.5 ± 33.3	20.1 ± 6.7	7.3 ± 2.7	2.1 ± 0.9
00TZ_A125	C	R5	24.0 ± 11.9	62.8 ± 11.8	27.7 ± 20.4	0.3 ± 0.1
BCF02	O	R5	6.9 ± 2.0	31.2 ± 3.3	9.3 ± 3.6	0.02 ± 0.01
92UG024	D	X4	30.2 ± 17.5	>100	42.9 ± 22.6	4.4 ± 1.6
BZ167/GS010	B	X4	22.1 ± 4.3	>100	25.3 ± 6.9	3.2 ± 2.3
MN/H9	A	X4	2.1 ± 1.7	>100	7.1 ± 6.9	0.5 ± 0.1
93/BR/020	F	X4/R5	7.6 ± 1.2	>100	39.5 ± 10.6	1.9 ± 0.9
97TH_NP1525	CRF01_AE	X4/R5	18.4 ± 1.2	>100	19.4 ± 2.8	1.6 ± 0.8

[a]All assays were performed in triplicate, and the data are expressed as the mean ± standard deviation. [b]CEMx174 5.25M7 cells expressing both CCR5 and CXCR4 on the surface were used in this study.

Table 4. Inhibitory Activity of CP12TAK against Infection by T20-Resistant HIV-1 Strains[a]

HIV-1 strain	EC_{50} (nM)[b]		
	T20	C34	CP12TAK
D36G[c]	4.31 ± 0.89	3.65 ± 0.56	0.66 ± 0.33
V38E/N42S[d]	261.22 ± 63.40 (60.6)	13.74 ± 6.28 (3.7)	0.39 ± 0.07 (0.6)
N42T/N43K[d]	672.86 ± 24.50 (156.1)	20.35 ± 5.13 (5.6)	0.52 ± 0.19 (0.8)
V38A/N42T[d]	655.63 ± 227.48 (152.1)	12.97 ± 6.64 (3.6)	0.55 ± 0.35 (0.8)

[a]The assay was performed in triplicate, and the data are expressed as the mean ± standard deviation. Values in parentheses indicate relative changes (*n*-fold) in the EC_{50} compared with the EC_{50} in the presence of the D36G substitution. [b]CEMx174 5.25M7 cells expressing both CCR5 and CXCR4 on the surface were used in this study. [c]T20-sensitive strain. [d]T20-resistant strain.

$1_{NL4\text{-}3(D36G)N42T/N43K}$ (EC_{50} = 673 nM), and HIV-$1_{NL4\text{-}3(D36G)V38A/N42T}$ (EC_{50} = 656 nM). Consistent with previous studies,[33] these T20-resistant HIV-1 variants also conferred cross-resistance to the C34 peptide. Impressively, CP12TAK retained high potency against these resistant viruses. The double mutations resulted in considerable high fold-changes of resistance to T20 and C34, but they had little effect on the potency of CP12TAK (Table 4).

CP12TAK Inhibited HIV-1 Infection by Interfering with Its Entry Step. A time-of-addition experiment was performed to determine the target stage of HIV-1 replication that is interfered by CP12TAK. The chimeric inhibitor was incubated with target cells during different intervals post-infection, and its inhibitory activity against HIV-1 BaL replication was measured. We found that addition of CP12TAK, together with virus, to the target cells had a profound inhibitory effect on HIV-1 replication (91% inhibition rate). However, a significantly decreased inhibitory effect was observed when CP12TAK was added to infected cells at 3 h or later (<37% inhibition rate), suggesting that CP12TAK is only effective at the entry stage of the viral lifecycle (Figure 3).

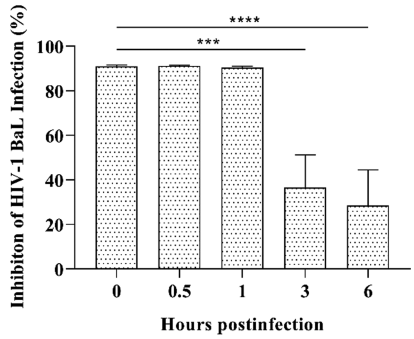

Figure 3. Time-of-addition experiment to clarify the stage at which dual-targeted inhibitors blocked HIV-1 infection. CP12TAK (20 nM) as a representative was added to CEMx174 5.25M7 cells at different time points postinfection of HIV-1 BaL strain. ***$p < 0.001$ and ****$p < 0.0001$ (two-way analysis of variance (ANOVA)). Data are presented as the mean ± standard deviations (n = 3).

CP12TAK Could Bind to the NHR Region of gp41. Subsequently, multiple biophysical and functional approaches were performed to understand the mechanism of action of these chimeras. We first determined whether CP12TAK could interact with the gp41 NHR target surrogate N36 peptide to form a complex, using native N-PAGE analysis, as described previously.[25,34] As shown in Figure 4A, N36 alone exhibited no band in the gel because it carries net positive charges and may move up and off the gel, which is consistent with previous observations.[25,34] Each of the peptides, including C34, CP12, and CP12TAK, displayed a band at different positions in the gel, depending on the net negative charge and molecular size of each one, while all mixtures of C34/N36, CP12/N36, and CP12TAK/N36 showed new bands at the upper position in the gel, indicating that CP12 and CP12TAK, like peptide C34, could form complexes. As analyzed by sedimentation velocity analysis (SVA), the sedimentation coefficient of the CP12TAK/N36 complex was 2.08 s, corresponding to 26.4 kDa, in agreement with the theoretical molecular mass of a CP12TAK/N36 6-HB (29.1 kDa) (Figure 4B). These results therefore suggested that CP12TAK could interact with N36 to form a 6-HB core structure. Next, circular dichroism (CD) experiments were performed to investigate the secondary structure and thermostability of the resulting CP12TAK/N36 hexamer (C34/N36 as a control). Peptides CP12TAK, C34, and N36 alone exhibited random coil structures. As expected, similar to C34, the chimeric inhibitor CP12TAK formed typical coiled coil after incubation with N36. CP12TAK and C34 interacted with N36 resulting in 58.7% and 75.5% α-helical content in the complex, respectively. Although CP12TAK induced slightly less α-helix content than C34,

https://doi.org/10.1021/acs.jmedchem.1c00781
J. Med. Chem. XXXX, XXX, XXX−XXX

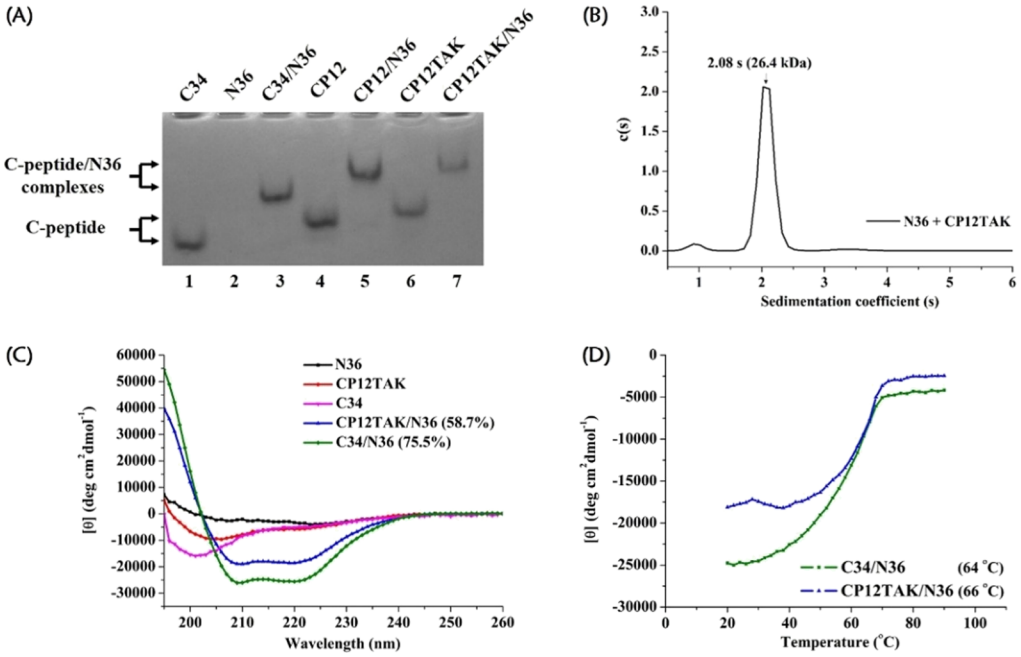

Figure 4. Determination of 6-HB formation between CP12TAK and N36. (A) Visualization of the binding of CP12TAK to the NHR peptide N36 by N-PAGE. (B) SVA of CP12TAK/N36 mixture. Sedimentation coefficient (s) and molecular mass (kDa) of each peak are indicated. The α-helicity (C) and thermostability (D) of CP12TAK/N36 6-HB. The α-helicity and *Tm* values are shown in parentheses. The final concentration of each peptide in PBS at 10 μM.

the CD thermal denaturation experiment showed a *Tm* value of 66 and 64 °C for CP12TAK/N36 and C34/N36 complexes, respectively, indicating that CP12TAK-based and C34-based 6-HBs have similar thermostability (Figure 4C,D).

CP12TAK Had Antagonistic Activity on RANTES-Induced Ca^{2+} Mobilization in CCR5-Expressing Cells. Having demonstrated the interaction of CP12TAK with the gp41 NHR-trimer at the prehairpin fusion-intermediate state, we next probed the binding of this dual-targeted inhibitor to cellular coreceptor CCR5. First, HIV-1 IIIB infection inhibition assay using MT-2 target cells expressing no CCR5 was carried out. We found that the potency enhancement of CP12TAK against X4 HIV-1 IIIB strain is target-cell coreceptor-dependent. When inhibiting HIV-1 IIIB infection on MT-2 cells expressing only CXCR4, CP12TAK behaved essentially the same as the 1:1 noncovalent mixture of C34 and TAK-220 (Table 5), which was different from its behavior in inhibiting HIV-1 IIIB infection in CEMx174 5.25M7 target cells expressing both CCR5 and CXCR4 (Figure 5). In contrast, C34, as the control, showed similar EC_{50} values on both CEMx174 5.25M7 and MT-2 target cells. To further investigate the coreceptor-targeting function of CP12TAK, we adapted a calcium (Ca^{2+}) mobilization assay to evaluate the antagonistic activity of the chimeric inhibitor on RANTES-induced Ca^{2+} mobilization via CCR5 in HEK293 cells. As shown in Figure 6, maraviroc, as a positive control, exhibited inhibitory activity against CCR5 and dose-dependently blocked the specific RANTES-induced intracellular Ca^{2+} flux with a half-maximal inhibitory concentration (IC_{50}) value of 0.82 nM. TAK-220 also showed activity toward CCR5 with an IC_{50} value of 1.49 nM. As expected, CP12TAK containing the coreceptor-inhibitor component maintained the potent antag-

Table 5. Anti-HIV-1_{IIIB} Activity of CP12TAK in MT-2 Cells[a]

HIV-1 strain (subtype, tropism)	EC_{50} (nM)[b]			
	CP12TAK	C34	TAK-220	C34/TAK-220[c]
IIIB (B, X4)	0.62 ± 0.33 (20.6)	1.34 ± 0.37 (0.8)	>50	0.63 ± 0.08 (0.2)

[a]The assay was performed in triplicate, and the data are expressed as the mean ± standard deviation. [b]HIV-1 IIIB strain infecting MT-2 cells expressing only CXCR4, but not CCR5, on the surface. Values in parentheses indicate relative changes (*n*-fold) that were calculated by dividing the EC_{50} of a compound when it was tested in MT-2 cells by that of the same compound tested in CEMx174 5.25M7 cells that has been shown in Table 2. [c]The molar ratio of C34/TAK-220 in combination was 1:1.

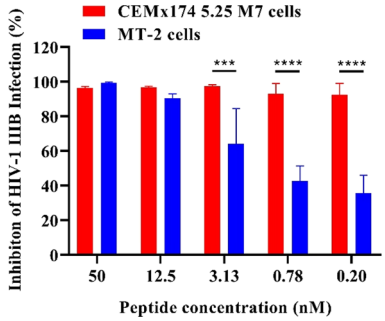

Figure 5. Antiviral potency of CP12TAK against X4-tropic HIV-1 IIIB infection in CEMx174 5.25M7 cells and MT-2 cells. Inhibitory activity of CP12TAK against X4-tropic HIV-1 IIIB infection in CEMx174 5.25M7 cells that express both CCR5 and CXCR4 and MT-2 cells which express only CXCR4 was compared. ***$p < 0.001$ and ****$p < 0.0001$ (two-way ANOVA). Experiments were performed in triplicate, and the data are expressed as mean ± standard deviations.

https://doi.org/10.1021/acs.jmedchem.1c00781
J. Med. Chem. XXXX, XXX, XXX−XXX

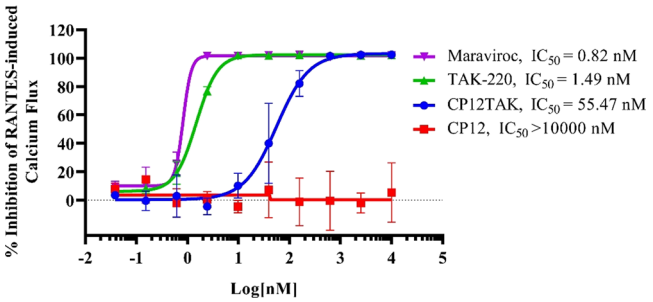

Figure 6. Concentration-dependent inhibition of RANTES-induced intracellular Ca^{2+} mobilization by HIV-1 inhibitors in HEK293 cells stably expressing CCR5. Fluo-4-loaded cells were treated with serial dilutions of HIV-1 inhibitors, including maraviroc, TAK-220, CP12TAK, and CP12, and then stimulated with RANTES at 4 nM. Experiments were performed in triplicate, and the data are expressed as means ± the standard deviations (error bar). Percent inhibition of the compounds and IC_{50} values were calculated.

onism of CCR5 with an IC_{50} value of 55.5 nM. Deletion of the CCR5 coreceptor-inhibitor portion of CP12TAK resulted in the loss of its inhibitory activity, that is, CP12 peptide exhibited no CCR5 antagonistic activity at the concentration up to 10 μM. These experiments provide evidence suggesting that CP12TAK could bind to the cellular CCR5 through its CCR5 antagonist pharmacophore.

DISCUSSION

HIV-1 entry proceeds through a cascade of three interdependent steps, including the attachment of the HIV-1 envelope glycoprotein gp120 to CD4 receptor on T-cells and macrophages, gp120 and coreceptor binding, and gp41-mediated membrane fusion. Each of these stages has afforded attractive targets for the development of viral entry inhibitors. Previous drug−drug combination studies have shown that using viral entry inhibitor combinations acting at two different steps, for example, the combination of a gp41-targeting fusion inhibitor with a gp120-targeting attachment inhibitor, or coreceptor antagonist, has resulted in strong synergistic inhibition of HIV-1 entry.[35−38] These findings encouraged us to engineer a novel entry inhibitor through incorporation of a small-molecule CCR5 antagonist, for example, TAK-220, and a peptide HIV-1 fusion inhibitor, such as C34, into one molecule. Strikingly, the covalent linkage of these two pharmacophores resulted in increased anti-HIV-1 potency of the chimeric inhibitors, and the change of the linker length affected their overall antiviral activity. Of note, CP12TAK peptide with a 12-unit PEG spacer was demonstrated as the most active inhibitor against infection of R5 HIV-1 BaL strain with an EC_{50} value of 0.03 nM, which is 39- and 306-fold higher than that of C34 alone and Tak-220 alone, respectively. We also demonstrated that covalent attachment led to a dramatic increase of the chimeric inhibitor's potency over that of the 1:1 (mol/mol) noncovalent mixture of C34/TAK-220 or CP12/TAK-220 that mimicked the molar ratio between inhibitors in the chimeric bifunctional compound. These data strongly suggest that HIV-1 fusion inhibitor C34 and CCR5 antagonist, when acting together, but on different targets within the same entry cascade, provide a synergistic antiviral effect.

To investigate whether the gp41 NHR-targeted fusion inhibitor moiety and small-molecule CCR5 antagonist portion within the bifunctional entry inhibitor indeed act on their targets accordingly, a series of mutations were made to CP12TAK, and the corresponding effects on inhibition of HIV-1 infection were evaluated. The N-terminal PBD truncation of CP12TAK into P26TAK (Table 1) leads to a dramatic loss of antiviral potency. Cocrystallization of C34 with its target N36 sequence has revealed that the PBD motif within the C34 peptide penetrates into the gp41 NHR primary pocket and plays a critical role in maintaining its inhibitory activity.[12] Thus, loss of biological activity of CP12TAK in the absence of PBD suggests that the C34 part of this chimeric inhibitor is also indispensable. Consistently, truncation of CP12TAK into CP12 resulted in remarkable reduction of antiviral activity by the loss of the CCR5 inhibitor moiety (Table 1). These structure−activity relationship (SAR) studies imply that increased antiviral potency results from both components attached as one molecule. Moreover, our biophysical studies with N-PAGE, SVA, and CD spectroscopy indicated that CP12TAK, like C34 peptide, could bind to the exposed grooves on the gp41 NHR-trimer to form heterologous 6-HB, thereby preventing HIV-1−cell membrane fusion. Using MT-2 cells expressing only CXCR4 as target cells, we observed the loss of synergistic potency of CP12TAK against HIV-1 IIIB infection, indicating that the chimera could bind to the CCR5 coreceptor. This finding was further confirmed by calcium flux assay. These observations from biophysical studies and functional experiments, combined with prior SAR analysis in CP12TAK, have demonstrated that each moiety in this bifunctional molecule maintains the capacity to interact with its specific target and, consequently, produce pharmacological responses that synergistically halt the cascade of HIV-1 fusion and entry. One hypothesis to explain the cooperative antiviral effects of two pharmacophores in one molecule is that blockage of the coreceptor via the CCR5 antagonist leads to delayed kinetics of the viral fusion process and increased its sensitivity to the C34 peptide.[39,40] Recently, numerous reports have shown that fusion inhibitor localization to membrane microdomains where fusion occurs via lipid conjugation can effectively enhance the inhibitory potency of these fusion-inhibitory peptides.[21,30,41] Therefore, another possible explanation is that membrane localization of CP12TAK by binding of the TAK-220 pharmacophore to the CCR5 coreceptor, much like lipids, such as cholesterol and fatty acids, raised the local concentration of the C34 peptide at the target site and thus increased the association rate for C34 binding to its viral NHR region target within the short-lived prehairpin intermediate of gp41. The third speculative reasoning is that the favorable entropic contribution could be responsible for the intramolecular cooperation of the two inhibitors.[42] In this scenario, when a fusion inhibitor and a CCR5 antagonist are tethered in a single molecule using a PEG12 linker, the smaller loss of entropy upon target binding compared to the sum of entropy cost resulted from binding of two separate components to their individual targets may account for their synergistically inhibited HIV-1 infection. A much looser PEG24 linker between C34 and TAK-220 resulted in a dramatic decrease in antiviral potency of CP24TAK, possibly because its large loss of entropy for target binding is similar to that of the unlinked combination of the individual inhibitors.

One possible concern over long-term administration of the CCR5 antagonist maraviroc is the coreceptor switch between X4-tropic HIV-1 strains and R5X4 dual-tropic viruses to gain entry and infect the host cells.[15,43] As expected, the CCR5 antagonist TAK-220 showed no inhibition at the concentration

https://doi.org/10.1021/acs.jmedchem.1c00781
J. Med. Chem. XXXX, XXX, XXX−XXX

as high as 100 nM against infection by either X4-tropic or dual-tropic viruses in CEMx174 5.25M7 cells that express both CCR5 and CXCR4 receptors. The C34 peptide is active because of its ability to bind the gp41 NHR region. When the CCR5 blocker TAK-220 was incorporated into the peptide, a 54-fold increase in potency against X4-tropic IIIB strain infection was noted in comparison to C34, but this synergism diminished in the mixture state. Further testing on X4 and R5 clinical isolates confirmed that CP12TAK was dramatically more potent than C34. One may question why this bifunctional entry inhibitor composed of one CCR5 antagonist linked to a fusion inhibitor is more effective in inhibiting X4-tropic and X4R5 dual-tropic strains than either of the components alone. Consistently, previous studies have reported that a chimeric HIV-1 entry inhibitor composed of a CCR5 natural ligand RANTES variant covalently linked to a gp41 peptide fusion inhibitor, designated 5P12-linker-C37, fully retains the anti-X4 activity of the fusion inhibitor, and this anti-X4 potency can be further enhanced when the target cells coexpress CCR5 on the surface.[44] Another bifunctional HIV-1 entry inhibitor named BFFI in which two peptide fusion inhibitors fused to the C-terminal ends of the heavy chain of a mAb targeting CCR5 also inhibited X4 HIV_{NL4-3} with dramatically increased potency in comparison to fusion inhibitor alone on target cell lines expressing both CCR5 and CXCR4 coreceptors.[45] Based on these observations, it can be speculated here that the dramatically increased antiviral efficacy of CP12TAK against X4-tropic HIV-1 on $CD4^+CCR5^+CXCR4^+$ cells could be explained by its CCR5 interaction. There have been reports showing that chemokine receptors CCR5 and CXCR4 form heterodimers on the cell surface.[46,47] Therefore, CP12TAK increases the potency of the fusion inhibitor moiety probably because of anchoring of the coreceptor portion of this hybrid molecule to CCR5. The localization to CCR5 on the host cell membrane brings the fusion inhibitor to its target in gp41 protein from X4-tropic HIV-1 who use nearby CXCR4 coreceptor for their entry. In accordance with this speculation, a noncovalent mixture of C34 and TAK-220 only exhibited anti-X4 activities at a similar level to their individual components alone on $CD4^+CCR5^+CXCR4^+$ cells. Furthermore, the chimeric inhibitor CP12TAK inhibited X4-tropic HIV-1 with antiviral activity similar to that observed for C34 alone in cell lines expressing only CXCR4 but not CCR5. CP12TAK was able to inhibit infection of $CD4^+CCR5^-CXCR4^+$ cells with X4-tropic HIV-1 IIIB, possibly because the small-molecule CCR5 inhibitor portion has a minimal steric hindrance to gp41 NHR target binding of the peptide fusion inhibitor, and consequently no adverse effects on the anti-HIV-1 activity of C34 were observed. Indeed, further investigation of the mechanisms of action of the chimeric inhibitor on X4- and R5/X4-tropic viruses is warranted.

Drug resistance is the major disadvantage for current clinical application of T20. It easily induces T20-resistant mutations in the GIV motif (residues 36 to 45 GIVQQQNNLL) in the gp41 NHR region.[26] C34 is much more potent in inhibiting T20-resistant strains, even though some of these strains still exhibit resistance to this PBD-containing peptide. To explain, it is possible that C34 also contains the GIV-motif-binding domain. Strikingly, CP12TAK has dramatically increased inhibition against infection of T20-resistant HIV-1 mutants. Chong et al. found that addition of an M-T hook to the N-terminus of C34 could allow it to effectively overcome the problem of T20 resistance.[48] Su et al. have designed an analogous peptide of HP23, HP23-E6-IDL, by adding an IDL (Ile-Asp-Leu) anchor to the C-terminus of the HP23 peptide. The newly designed peptide exhibited high potency against HP23-resistant strains.[49] These findings are consistent with that seen for CP12TAK, suggesting construction of molecules that can hit multiple target sites could significantly improve a peptide's resistance profile. In addition to efficiently inhibiting the existing inhibitor-resistant HIV-1 variants, an ideal next-generation HIV-1 entry inhibitor should possess a high genetic barrier to resistance. Compared with T20, C34 is less susceptible to the evolution of resistant viruses.[48] In viral selection experiments, viruses resistant to TAK-220 could not yet be isolated in *vitro*.[50] Moreover, extensive studies have shown that incorporation of an extra motif, for example, M-T hook structure, to C34, or sifuvirtide, could significantly increase the genetic barrier of inhibitors to the development of drug resistance.[48] Thus, we expect that CP12TAK may lead to delayed drug-resistant mutations in HIV-1 variants.

Overall, CP12TAK, as an outstanding MTDL lead compound, has exquisite potency against R5-tropic, X4-tropic, and dual-tropic HIV-1 strains, and it is substantially greater than that of its individual components alone or in combination. Moreover, the incorporation of two inhibitors into one molecule could overcome some drawbacks of the parent single-target drugs, for example, the treatment failures of the CCR5 antagonist associated with patients infected by non-R5 viruses and rapid emergence of viral strains resistant to T20. The current emerging severe acute respiratory syndrome coronavirus 2 (SARS-CoV-2) merits mention in the context of our *de novo* dual-targeted compound. In particular, the 6-HB inhibition strategy has been successfully applied to SARS-CoV-2, which utilizes a class I fusion protein, similar to that of HIV-1, for the discovery and development of effective fusion inhibitors.[51] In addition to inhibition of the cascade of conformational changes of fusion proteins, interference of the priming of SARS-CoV-2 spike protein by blocking transmembrane protease serine 2 also opens a new avenue for preventing the entry process between viral and cellular membranes.[52] Therefore, based on the results obtained from the present study, combined with these significant advances in the development of SARS-CoV-2 entry inhibitors, the approach of making MTDLs by linking two active ligands together could be proposed as a promising strategy for the discovery of SARS-CoV-2 entry inhibitors with reliable efficacy and safety.

Recently, a series of multitargeted compounds has been designed via linking together a peptide fusion inhibitor and a CCR5-specific monoclonal antibody or variants of natural ligands which interfere with gp120-CCR5 binding.[44,45] Compared with these biologics-based dual-binding site entry inhibitors, CP12TAK has several strengths. First, CP12TAK can be easily synthesized, thus having lower production cost than chimeric molecules containing large proteins. Second, CP12TAK is very amenable to site-specific modification to discover and develop new lead compounds with a novel scaffold and higher potency. Third, CP12TAK can inhibit X4-tropic viruses on cell lines expressing only the CXCR4 coreceptor, whereas the monoclonal antibody-based entry inhibitors can only exert an antiviral effect on cells coexpressing CCR5. Fourth, small-molecule CCR5 antagonists, unlike natural ligands for CCR5, would not induce cell signaling or internalization,[43] thus potentially lessening the

https://doi.org/10.1021/acs.jmedchem.1c00781
J. Med. Chem. XXXX, XXX, XXX−XXX

risks associated with the use of CCR5 natural ligand variants as coreceptor pharmacophores in dual-functional drug design.

CONCLUSIONS

In conclusion, we provide an example of MTDL design strategy for creating dual-targeting HIV-1 entry inhibitors via combining a gp41 peptide fusion inhibitor and a small-molecule CCR5 antagonist into one compound. We demonstrated that this dual-functional compound preserved the specific targeting properties of the two distinct pharmacophores and, at the same time, exhibited highly potent antiviral activity against laboratory-adapted HIV-1 strains and primary HIV-1 isolates with diverse subtypes and T20-resistant mutants. Also, the exceptional potency of the dual-targeting ligands benefits from synergy between the coreceptor antagonist and gp41 inhibitor. Overall, our designed CP12TAK provides a therapeutic lead molecule for developing new anti-HIV-1 drugs. Moreover, this work highlights the development of MTDLs for the treatment of complex infectious diseases caused by enveloped viruses, such as HIV, MERS-CoV, and SARS-CoV-2.

EXPERIMENTAL SECTION

Chemistry. Unless otherwise stated, all materials used were commercially obtained and used as supplied. Thin layer chromatography was performed on silica gel GF_{254} plates. Silica gel (200−300 mesh) from Qingdao Haiyang Chemical Company was used for column chromatography. ^{1}H (400 MHz) and ^{13}C (100 MHz) NMR spectra were measured on a JNM-ECA-400 spectrometer using TMS as the internal standard. Chemical shifts for the proton-magnetic-resonance (^{1}H NMR) spectra were quoted in parts per million (ppm) and referenced to the signals of residual chloroform (7.29 ppm) or methanol (3.30 ppm). All ^{13}C NMR spectra were reported in ppm relative to deuterochloroform (77.00 ppm) or methanol (49.00 ppm). For small molecules, mass spectra (MS) were measured on an API-150 mass spectrometer with an electrospray ionization source from ABI Inc. For compounds tested in biological assay, the purity of each compound was confirmed to be ≥95% by analytical reversed-phase high-performance liquid chromatography (RP-HPLC) (Shimadzu analytical HPLC system). Such information is provided in the Supporting Information (Tables S2 and S3). The molecular weight of the peptides was characterized by matrix-assisted laser desorption ionization−time-of-flight mass spectrometry (Autoflex III, Bruker Daltonics Inc., Billerica, MA).

Synthesis of Compound 1. To a solution of 1-acetylpiperidine-4-carboxylic acid (1 g, 5.84 mmol) in THF (15 mL) was added N,N′-carbonyldiimidazole (1.42 g, 8.76 mmol) at room temperature. After stirring at room temperature for 4 h, 3-chloro-4-methylaniline was added, and the mixture was stirred for 24 h. The mixture was concentrated in vacuo, and the residue was diluted with dichloromethane (DCM). The organic layer was washed with aqueous $NaHCO_3$ and brine, dried over $MgSO_4$, and concentrated in vacuo. The residue was purified by column chromatography (EtOAc/MeOH 50: 1 to 30: 1) to give 1.41 g (82%) of **1** as a white solid. ^{1}H NMR (400 MHz, $CDCl_3$) δ 8.11 (b, 1H), 7.62 (d, J = 2.2 Hz, 1H), 7.30 (dd, J = 8.2 Hz, J = 2.2 Hz, 1H), 7.12 (d, J = 8.2 Hz, 1H), 4.56 (d, J = 13.5 Hz, 1H), 3.87 (d, J = 13.5 Hz, 1H), 3.11 (t, J = 12.4 Hz, 1H), 2.69 (t, J = 12.4 Hz, 1H), 2.52 (m, 1H), 2.31 (s, 3H), 2.11 (s, 3H), 1.95 (m, 2H), 1.79 (m, 2H). ^{13}C NMR (100 MHz, $CDCl_3$) δ 172.47, 169.17, 135.72, 134.33, 131.84, 130.93, 120.54, 118.25, 45.74, 43.57, 41.00, 28.70, 28.45, 21.34, 19.39. MS (m/z): calcd for $C_{15}H_{19}ClN_2O_2$, 294.11. LC−MS (m/z (rel intens)): 295.11 (M + H, 100).

Synthesis of Compound 2. To an ice-cooled stirred solution of **1** (1.0 g, 2.8 mmol) in DMF (15 mL) was added NaH (60% in oil, 0.70 g, 29.2 mmol), and the mixture was stirred at 0 °C for 30 min. To the mixture was added 1-bromo-3-chloropropane (0.89 g, 5.7 mmol), and the mixture was stirred at room temperature for 1 h. The mixture was diluted with water (50 mL) and extracted with EtOAc (3 × 50 mL). The organic layer was washed with brine (3 × 50 mL) and concentrated in vacuo. The residue was purified by column chromatography on silica gel (EtOAc/MeOH 1:0 to 9:1) followed by recrystallization from EtOAc/Et_2O to afford **2** (0.65 g, 63%) as a white solid. ^{1}H NMR (400 MHz, $CDCl_3$) δ 7.32 (d, J = 8.0 Hz, 1H), 7.19 (d, J = 2.2 Hz, 1H), 6.99 (dd, J = 8.0 Hz, J = 2.2 Hz, 1H), 4.52 (d, J = 13.2 Hz, 1H), 3.77 (t, J = 6.6 Hz, 3H), 3.52 (t, J = 6.6 Hz, 2H), 2.85 (t, J = 13.1 Hz, 1H), 2.43 (s, 3H), 2.77 (m, 2H), 2.05 (s, 3H), 2.00 (m, 2H), 1.75 (m, 4H). ^{13}C NMR (100 MHz, $CDCl_3$) δ 174.10, 168.68, 140.77, 135.62, 135.29, 132.00, 128.29, 126.16, 47.52, 45.38, 42.17, 40.54, 39.19, 30.68, 28.70, 28.19, 21.26, 19.70. MS (m/z): calcd for $C_{18}H_{24}Cl_2N_2O_2$, 370.12. LC−MS (m/z (rel intens)): 371.12 (M + H, 100).

Synthesis of Compound 3. Using literature procedures,[27] compound **3** was prepared (70.4% yield). ^{1}H NMR (400 MHz, $CDCl_3$) δ 7.99 (d, J = 7.7 Hz, 2H), 7.26 (d, J = 7.7 Hz, 2H), 6.37 (s, 1H), 3.91 (s, 3H), 3.52 (t, J = 5.8 Hz, 2H), 3.41 (t, J = 5.8 Hz, 2H), 2.46 (t, J = 5.8 Hz, 2H), 2.35 (t, J = 5.8 Hz, 2H), 1.48 (s, 9H). ^{13}C NMR (100 MHz, $CDCl_3$) δ 166.89, 154.67, 142.18, 140.62, 129.48, 128.77, 127.90, 123.83, 79.62, 51.99, 45.25, 44.39, 36.26, 29.29, 28.39. MS (m/z): calcd for $C_{19}H_{25}NO_4$, 331.18. LC−MS (m/z (rel intens)): 354.16 (M + Na, 27).

Synthesis of Compound 4. Using literature procedures,[27] compound **4** was prepared (94.9% yield). ^{1}H NMR (400 MHz, $CDCl_3$) δ 9.49 (b, 1H), 9.04 (b, 1H), 7.97 (d, J = 7.9 Hz, 2H), 7.21 (d, J = 7.9 Hz, 2H), 3.90 (s, 3H), 3.35 (m, J = 12.8 Hz, 2H), 2.82 (m, J = 12.4 Hz, 2H), 2.65 (t, J = 6.7 Hz, 2H), 1.82 (d, J = 12.4 Hz, 3H), 1.60 (m, 2H). ^{13}C NMR (100 MHz, $CDCl_3$) δ 166.89, 144.30, 129.84, 128.99, 128.50, 52.04, 43.90, 42.28, 35.93, 28.47. MS (m/z): calcd for $C_{14}H_{19}NO_2$, 233.14. LC−MS (m/z (rel intens)): 234.13 (M + H, 100).

Synthesis of Compound 5. To a mixture of compound **2** (1.38 g, 3.72 mmol), compound **4** (1.0 g, 3.72 mmol), and K_2CO_3 (2.05 g, 14.8 mmol) in DMF/acetonitrile (80 mL, 1:1, v/v) was added KI (0.62 mg, 4.5 mmol), and the mixture was stirred at reflux for 12 h. After cooling to room temperature, the mixture was filtered, and the filtrate was concentrated in a vacuo. The residue was diluted with EtOAc, washed with water and brine, dried with $MgSO_4$, filtered, and concentrated in vacuo. Purification silica gel chromatography (EtOAc/MeOH 1: 0 to 5: 1) afforded **9** as a white foam (0.63 g, 30.3% yield). ^{1}H NMR (400 MHz, $CDCl_3$) δ 11.14 (b, 1H), 9.12 (b, 1H), 7.97 (d, J = 7.7 Hz, 2H), 7.32 (d, J = 8.0 Hz, 1H), 7.21 (m, 3H), 7.03 (dd, J = 8.0 Hz, J = 2.2 Hz, 1H), 4.52 (d, J = 13.3 Hz, 1H), 3.90 (s, 3H), 3.79 (m, 2H), 3.64 (b, 3H), 3.07 (m, 2H), 2.89 (m, 1H), 2.65 (m, 4H), 2.41 (b, 5H), 2.08 (s, 3H), 1.99 (m, 2H), 1.86 (m, 2H), 1.74 (m, 6H). ^{13}C NMR (100 MHz, $CDCl_3$) δ 174.95, 169.79, 166.83, 160.95, 160.58, 144.15, 139.72, 137.29, 135.58, 132.28, 129.78, 128.92, 128.45, 127.88, 126.24, 117.09, 114.21, 54.82, 53.25, 52.97, 51.97, 46.44, 45.47, 41.81, 40.88, 38.92, 35.81, 29.00, 28.61, 27.95, 22.68, 20.63, 19.63. MS (m/z): calcd for $C_{32}H_{42}ClN_3O_4$, 267.29. LC−MS (m/z (rel intens)): 568.28 (M + H, 100).

Synthesis of Compound TAK. To a stirred solution of compound **5** (1.5 g, 2.65 mmol) in dioxane (15 mL) was added 1 M NaOH (15 mL). The mixture was stirred at room temperature for 1 h, quenched with 1 M HCl (5 mL), extracted with DCM (15 mL × 3), dried, filtered, and concentrated. Purification by silica gel chromatography (1:1 EtOAc/methanol) afforded TAK as a white solid (0.94 g, 64.1% yield). ^{1}H NMR (400 MHz, CD_3OD) δ 7.96 (d, J = 8.2 Hz, 2H), 7.45 (m, 2H), 7.30 (d, J = 8.2 Hz, 2H), 7.22 (dd, J = 2.1 Hz, 1H), 4.43 (d, J = 13.4 Hz, 1H), 3.87 (d, J = 13.4 Hz, 1H), 3.77 (m, 2H), 3.56 (d, J = 12.2 Hz, 2H), 3.09 (t, J = 7.7 Hz, 2H), 2.93 (t, J = 12.2 Hz, 3H), 2.70 (d, J = 6.6 Hz, 2H), 2.51 (m, 1H), 2.41 (s, 3H), 2.39 (m, 1H), 2.04 (s, 3H), 1.96 (m, 5H), 1.71 (m, 3H), 1.59 (m, 3H). ^{13}C NMR (100 MHz, CD_3OD) δ 177.66, 171.90, 170.20, 146.63, 142.11, 138.85, 136.94, 134.03, 131.45, 130.81, 130.60, 130.07, 128.35, 55.92, 54.51, 48.18, 47.14, 43.30, 42.32, 41.20, 37.00, 31.03, 30.36, 29.80, 24.05, 21.61, 20.26. MS (m/z): calcd for $C_{31}H_{40}ClN_3O_4$, 553.27. LC−MS (m/z (rel intens)): 554.26 (M + H, 100).

https://doi.org/10.1021/acs.jmedchem.1c00781
J. Med. Chem. XXXX, XXX, XXX−XXX

Peptide Synthesis. Peptides were synthesized using standard Fmoc solid-phase synthesis techniques with a CS biopolypeptide synthesizer. Rink Amide resin, with a resin loading of 0.53 mmol/g, was selected as the solid support. DMF, DCM, *N*-methyl-2-pyrrolidone, methanol, piperidine, and other reagents used in the reaction process were anhydrous reagents or dried prior to use. The template peptides containing a deprotected lysine residue at their C-terminus required a special deprotection step (four 3-min washes of 2% hydrazinehydrate in DMF). This enabled the conjugation of a small-molecule moiety, which was performed by the addition of three equivalents of small molecules, three equivalents of HBTU, and six equivalents of DIEA in DMF to the resin followed by stirring for 2 h. The peptides were cleaved from the resin and deprotected with reagent K, which contained 85% trifluoroacetic acid, 5% thioanisole, 5% *m*-cresol, and 5% water. The carboxyl termini were amidated upon cleavage from the resin, and the amino termini were capped with acetic acid anhydride. All crude peptides were purified by RP-HPLC (Shimadzu preparative HPLC system), and the purity of each peptide was confirmed to be ≥95% by analytical RP-HPLC (Shimadzu analytical HPLC system). The molecular weight of the peptides was characterized by matrix-assisted laser desorption ionization−time-of-flight mass spectrometry (Autoflex III, Bruker Daltonics Inc., Billerica, MA).

Inhibition of HIV-1 Infection. Inhibitory activities of peptides against HIV-1 infection were determined as previously described.[49,53] Briefly, 100 $TCID_{50}$ HIV-1 strains were infected with 10^4 CEMx174 5.25M7 or MT-2 cells at 37 °C overnight with tested compounds that were diluted with fetal bovine serum (FBS)-free RPMI 1640 medium. The medium was replaced with fresh RPMI 1640 medium containing 10% FBS the next morning. After an additional 6 days for CEMx174 5.25M7 cells and 3 days for MT-2 cells, the culture supernatants from each well were mixed with equal volumes of 5% Triton X-100. P24 antigen was detected using ELISA assay. The IC_{50} values were calculated using CalcuSyn software.[54]

Cytotoxicity Assay. Serial dilutions of CP12TAK were mixed with CEMx174 5.25M7 cells. Then the culture medium was replaced with fresh RPMI 1640 medium with 10% FBS 10 h later. The cytotoxicity of CP12TAK was tested after an additional 48 h using the Cell Counting Kit-8 (Dojindo, Japan).

Native-PAGE. Peptides at a final concentration of 50 μM, including the N- and C-terminal free peptides, as well as their equimolar mixtures, were dissolved in PBS (1×, pH 7.4) and incubated at 37 °C for 30 min. After mixing the above peptides with Tris-glycine native sample buffer (BioRad, Hercules, CA) in a 1:1 ratio, the samples were loaded (20 μL in each well) onto 10% Tris-glycine gels. Gel electrophoresis was run under a constant voltage of 120 V at room temperature for 4 h. The obtained gel was then stained with Coomassie Blue R250. The images were taken using a ChampGel 6000 Imaging System (Sage Creation Ltd., Beijing, China).

SVA. SVA was performed using a Proteomelab XL-A/XL-I analytical ultracentrifuge (Beckman Coulter, Fullerton, CA) equipped with a three-channel cell and an An-60 Ti rotor. All samples were prepared at a final concentration of 150 μM in PBS (1×, pH 7.4). The C-peptides/N36 mixtures were incubated at 37 °C for 30 min and were initially scanned at 3000 rpm for 10 min. Data were obtained at a wavelength of 280 nm after centrifugation at 60,000 rpm and 20 °C for 7 h. Weight-averaged molecular weights were calculated and fitted by processing with the SEDFIT program.

CD Spectroscopy. The C-peptides and N36 were dissolved in PBS (1×, pH 7.4) and ddH_2O, respectively, at a concentration of 10 μM. The equimolar mixtures were incubated at 37 °C for 30 min at a final concentration of 10 μM. The CD spectra were recorded on a MOS-450 system (BioLogic, Claix, France) with the following conditions: temperature, 4 °C; wavelength, 190−260 nm; resolution, 0.1 nm; path length, 0.1 cm; response time, 4.0 s; and scanning speed, 50 nm/min. The obtained results were processed to obtain the mean residue ellipticity. A mean residue ellipticity $[\theta]$ of −33,000° cm^2/dmol at a wavelength of 222 nm was considered to be 100% α-helicity. Thermal denaturation was monitored at 222 nm by the ellipticity change by applying a thermal gradient of 2 °C/min from 20 to 90 °C.

Calcium Mobilization Assay. Intracellular calcium fluxes were measured with the FLIPR Tetra system. HEK293 cells stably expressing Gα15 and CCR5 were seeded onto 384-well plates and incubated at 37 °C in 5% CO_2 overnight. Cells were loaded with 4 μM Fluo-4 Direct (Invitrogen, Cat# F10471) in Assay Buffer [Hanks' balanced salt solution (HBSS):HEPES = 49:1, v/v] and incubated for 50 min at 37 °C with 5% CO_2 followed by an incubation for 10 min at room temperature. After washing, 10 μL HBSS containing various concentrations of testing compounds was added. After incubation at room temperature for 10 min, 10 μL HBSS containing RANTES-(CCL5) (final concentration 4 nM) was added to the cell plate, and the intracellular calcium change was recorded at an excitation wavelength of 490 nm and an emission wavelength of 515 nm. The IC_{50} values of the compounds were determined with GraphPad Prism software by constructing their dose−response curves.

■ ASSOCIATED CONTENT

Supporting Information

The Supporting Information is available free of charge at https://pubs.acs.org/doi/10.1021/acs.jmedchem.1c00781.

HPLC method used for the purification of peptide compounds; HPLC method used for the analysis of peptide compounds; potential cytotoxicity of CP12TAK on CEMx174 5.25M7 and MT-2 cells; MALDI-TOF-MS and Analytical HPLC of designed peptides; ^1H and ^{13}C NMR spectra of small-molecule compounds; and ESI-TOF-MS spectra of small-molecule compounds (PDF)

Molecular formula strings (CSV)

■ AUTHOR INFORMATION

Corresponding Authors

Chao Wang − *State Key Laboratory of Toxicology and Medical Countermeasures, Beijing Institute of Pharmacology and Toxicology, Beijing 100850, China;* orcid.org/0000-0002-7673-0638; Phone: 86-10-6693-0640; Email: chaow301@sina.com; Fax: 86-10-6821-1656

Yang Liu − *Key Laboratory of Structure-based Drug Design & Discovery of Ministry of Education, School of Pharmaceutical Engineering, Shenyang Pharmaceutical University, Shenyang 110016, China;* orcid.org/0000-0002-9284-1944; Phone: 86-24-4352-0227; Email: y.liu@syphu.edu.cn

Lu Lu − *Key Laboratory of Medical Molecular Virology (MOE/NHC/CAMS), School of Basic Medical Sciences and Shanghai Public Health Clinical Center, Shanghai Institute of Infectious Diseases and Biosecurity, Fudan University, Shanghai 200032, China*; Phone: 86-21-5423-7671; Email: lul@fudan.edu.cn; Fax: 86-21-5423-7465

Shibo Jiang − *Key Laboratory of Medical Molecular Virology (MOE/NHC/CAMS), School of Basic Medical Sciences and Shanghai Public Health Clinical Center, Shanghai Institute of Infectious Diseases and Biosecurity, Fudan University, Shanghai 200032, China;* orcid.org/0000-0001-8283-7135; Phone: 86-21-5423-7673; Email: shibojiang@fudan.edu.cn; Fax: 86-21-5423-7465

Authors

Xinling Wang − *Key Laboratory of Medical Molecular Virology (MOE/NHC/CAMS), School of Basic Medical Sciences and Shanghai Public Health Clinical Center, Shanghai Institute of Infectious Diseases and Biosecurity, Fudan University, Shanghai 200032, China*

https://doi.org/10.1021/acs.jmedchem.1c00781
J. Med. Chem. XXXX, XXX, XXX−XXX

Huan Wang − *State Key Laboratory of Toxicology and Medical Countermeasures, Beijing Institute of Pharmacology and Toxicology, Beijing 100850, China*

Jing Pu − *Key Laboratory of Medical Molecular Virology (MOE/NHC/CAMS), School of Basic Medical Sciences and Shanghai Public Health Clinical Center, Shanghai Institute of Infectious Diseases and Biosecurity, Fudan University, Shanghai 200032, China*

Qing Li − *State Key Laboratory of Toxicology and Medical Countermeasures, Beijing Institute of Pharmacology and Toxicology, Beijing 100850, China*

Jiahui Li − *Key Laboratory of Structure-based Drug Design & Discovery of Ministry of Education, School of Pharmaceutical Engineering, Shenyang Pharmaceutical University, Shenyang 110016, China*

Complete contact information is available at: https://pubs.acs.org/10.1021/acs.jmedchem.1c00781

Author Contributions

[‖]C.W. and X.W. contributed equally to this work.

Notes

The authors declare no competing financial interest.

■ ACKNOWLEDGMENTS

This research was supported, in part, by grants from the National Natural Science Foundation of China (21877127 to C.W.; 81630090 to S.J.; and 81822045 to L.L.) and Shanghai Clinical Research Center for Infectious Disease (HIV/AIDS) (20MC1920100).

■ ABBREVIATIONS

CHR, C-terminal heptad repeat; NHR, N-terminal heptad repeat; 6-HB, six-helix bundle.

■ REFERENCES

(1) Bottegoni, G.; Favia, A. D.; Recanatini, M.; Cavalli, A. The role of fragment-based and computational methods in polypharmacology. *Drug Discovery Today* **2012**, *17*, 23−34.

(2) Rosini, M.; Simoni, E.; Minarini, A.; Melchiorre, C. Multi-target design strategies in the context of Alzheimer's disease: acetylcholinesterase inhibition and NMDA receptor antagonism as the driving forces. *Neurochem. Res.* **2014**, *39*, 1914−1923.

(3) Fumakia, M.; Yang, S.; Gu, J.; Ho, E. A. Protein/peptide-based entry/fusion inhibitors as anti-HIV therapies: challenges and future direction. *Rev. Med. Virol.* **2016**, *26*, 4−20.

(4) Maeda, K.; Das, D.; Kobayakawa, T.; Tamamura, H.; Takeuchi, H. Discovery and development of anti-HIV therapeutic agents: progress towards improved HIV medication. *Curr. Top. Med. Chem.* **2019**, *19*, 1621−1649.

(5) Zhan, P.; Pannecouque, C.; De Clercq, E.; Liu, X. Anti-HIV drug discovery and development: current innovations and future trends. *J. Med. Chem.* **2016**, *59*, 2849−2878.

(6) Caplan, M. R.; Daar, E. S.; Corado, K. C. Next generation fixed dose combination pharmacotherapies for treating HIV. *Expert Opin. Pharmacother.* **2018**, *19*, 589−596.

(7) Zhou, J.; Jiang, X.; He, S.; Jiang, H.; Feng, F.; Liu, W.; Qu, W.; Sun, H. Rational design of multitarget-directed ligands: strategies and emerging paradigms. *J. Med. Chem.* **2019**, *62*, 8881−8914.

(8) Simoni, E.; Daniele, S.; Bottegoni, G.; Pizzirani, D.; Trincavelli, M. L.; Goldoni, L.; Tarozzo, G.; Reggiani, A.; Martini, C.; Piomelli, D.; Melchiorre, C.; Rosini, M.; Cavalli, A. Combining galantamine and memantine in multitargeted, new chemical entities potentially useful in Alzheimer's disease. *J. Med. Chem.* **2012**, *55*, 9708−9721.

(9) Kazmierski, W. M.; Kenakin, T. P.; Gudmundsson, K. S. Peptide, peptidomimetic and small-molecule drug discovery targeting HIV-1 host-cell attachment and entry through gp120, gp41, CCR5 and CXCR4. *Chem. Biol. Drug Des.* **2006**, *67*, 13−26.

(10) de Feo, C.; Weiss, C. Escape from human immunodeficiency virus type 1 (HIV-1) entry inhibitors. *Viruses* **2012**, *4*, 3859−3911.

(11) Lu, M.; Blacklow, S. C.; Kim, P. S. A trimeric structural domain of the HIV-1 transmembrane glycoprotein. *Nat. Struct. Biol.* **1995**, *2*, 1075−1082.

(12) Chan, D. C.; Fass, D.; Berger, J. M.; Kim, P. S. Core structure of gp41 from the HIV envelope glycoprotein. *Cell* **1997**, *89*, 263−273.

(13) Dorr, P.; Westby, M.; Dobbs, S.; Griffin, P.; Irvine, B.; Macartney, M.; Mori, J.; Rickett, G.; Smith-Burchnell, C.; Napier, C.; Webster, R.; Armour, D.; Price, D.; Stammen, B.; Wood, A.; Perros, M. Maraviroc (UK-427,857), a potent, orally bioavailable, and selective small-molecule inhibitor of chemokine receptor CCR5 with broad-spectrum anti-human immunodeficiency virus type 1 activity. *Antimicrob. Agents Chemother.* **2005**, *49*, 4721−4732.

(14) Palani, A.; Tagat, J. R. Discovery and development of small-molecule chemokine coreceptor CCR5 antagonists. *J. Med. Chem.* **2006**, *49*, 2851−2857.

(15) Perry, C. M. Maraviroc: a review of its use in the management of CCR5-tropic HIV-1 infection. *Drugs* **2010**, *70*, 1189−1213.

(16) Skerlj, R. T.; Bridger, G. J.; Kaller, A.; McEachern, E. J.; Crawford, J. B.; Zhou, Y.; Atsma, B.; Langille, J.; Nan, S.; Veale, D.; Wilson, T.; Harwig, C.; Hatse, S.; Princen, K.; De Clercq, E.; Schols, D. Discovery of novel small molecule orally bioavailable C-X-C chemokine receptor 4 antagonists that are potent inhibitors of T-tropic (X4) HIV-1 replication. *J. Med. Chem.* **2010**, *53*, 3376−3388.

(17) Wild, C.; Oas, T.; McDanal, C.; Bolognesi, D.; Matthews, T. A synthetic peptide inhibitor of human immunodeficiency virus replication: correlation between solution structure and viral inhibition. *Proc. Natl. Acad. Sci. U. S. A.* **1992**, *89*, 10537−10541.

(18) Jiang, S.; Lin, K.; Strick, N.; Neurath, A. R. HIV-1 inhibition by a peptide. *Nature* **1993**, *365*, 113.

(19) Wild, C. T.; Shugars, D. C.; Greenwell, T. K.; McDanal, C. B.; Matthews, T. J. Peptides corresponding to a predictive alpha-helical domain of human immunodeficiency virus type 1 gp41 are potent inhibitors of virus infection. *Proc. Natl. Acad. Sci. U. S. A.* **1994**, *91*, 9770−9774.

(20) Lalezari, J. P.; Henry, K.; O'Hearn, M.; Montaner, J. S.; Piliero, P. J.; Trottier, B.; Walmsley, S.; Cohen, C.; Kuritzkes, D. R.; Eron, J. J.; Chung, J.; DeMasi, R.; Donatacci, L.; Drobnes, C.; Delehanty, J.; Salgo, M. Enfuvirtide, an HIV-1 fusion inhibitor, for drug-resistant HIV infection in North and South America. *N. Engl. J. Med.* **2003**, *348*, 2175−2185.

(21) Pu, J.; Wang, Q.; Xu, W.; Lu, L.; Jiang, S. Development of protein- and peptide-based HIV entry inhibitors targeting gp120 or gp41. *Viruses* **2019**, *11*, 705.

(22) Vigant, F.; Santos, N. C.; Lee, B. Broad-spectrum antivirals against viral fusion. *Nat. Rev. Microbiol.* **2015**, *13*, 426−437.

(23) Zhu, J. D.; Meng, W.; Wang, X. J.; Wang, H. C. Broad-spectrum antiviral agents. *Front. Microbiol.* **2015**, *6*, 517.

(24) Xu, W.; Pu, J.; Su, S.; Hua, C.; Su, X.; Wang, Q.; Jiang, S.; Lu, L. Revisiting the mechanism of enfuvirtide and designing an analog with improved fusion inhibitory activity by targeting triple sites in gp41. *AIDS* **2019**, *33*, 1545−1555.

(25) Zhang, X.; Ding, X.; Zhu, Y.; Chong, H.; Cui, S.; He, J.; Wang, X.; He, Y. Structural and functional characterization of HIV-1 cell fusion inhibitor T20. *AIDS* **2019**, *33*, 1−11.

(26) Cai, L.; Jiang, S. Development of peptide and small-molecule HIV-1 fusion inhibitors that target gp41. *ChemMedChem* **2010**, *5*, 1813−1824.

(27) Imamura, S.; Ichikawa, T.; Nishikawa, Y.; Kanzaki, N.; Takashima, K.; Niwa, S.; Iizawa, Y.; Baba, M.; Sugihara, Y. Discovery of a piperidine-4-carboxamide CCR5 antagonist (TAK-220) with highly potent anti-HIV-1 activity. *J. Med. Chem.* **2006**, *49*, 2784−2793.

(28) Liu, T.; Weng, Z.; Dong, X.; Chen, L.; Ma, L.; Cen, S.; Zhou, N.; Hu, Y. Design, synthesis and biological evaluation of novel

piperazine derivatives as CCR5 antagonists. *PLoS One* **2013**, *8*, No. e53636.
(29) Ingallinella, P.; Bianchi, E.; Ladwa, N. A.; Wang, Y. J.; Hrin, R.; Veneziano, M.; Bonelli, F.; Ketas, T. J.; Moore, J. P.; Miller, M. D.; Pessi, A. Addition of a cholesterol group to an HIV-1 peptide fusion inhibitor dramatically increases its antiviral potency. *Proc. Natl. Acad. Sci. U. S. A.* **2009**, *106*, 5801−5806.
(30) Chong, H.; Wu, X.; Su, Y.; He, Y. Development of potent and long-acting HIV-1 fusion inhibitors. *AIDS* **2016**, *30*, 1187−1196.
(31) Chong, H.; Xue, J.; Xiong, S.; Cong, Z.; Ding, X.; Zhu, Y.; Liu, Z.; Chen, T.; Feng, Y.; He, L.; Guo, Y.; Wei, Q.; Zhou, Y.; Qin, C.; He, Y. A lipopeptide HIV-1/2 fusion inhibitor with highly potent *in vitro*, *ex vivo*, and *in vivo* antiviral activity. *J. Virol.* **2017**, *91*, No. e00288-17.
(32) Bailey, C. M.; Sullivan, T. J.; Iyidogan, P.; Tirado-Rives, J.; Chung, R.; Ruiz-Caro, J.; Mohamed, E.; Jorgensen, W. L.; Hunter, R.; Anderson, K. S. Bifunctional inhibition of human immunodeficiency virus type 1 reverse transcriptase: mechanism and proof-of-concept as a novel therapeutic design strategy. *J. Med. Chem.* **2013**, *56*, 3959−3968.
(33) Chong, H.; Yao, X.; Sun, J.; Qiu, Z.; Zhang, M.; Waltersperger, S.; Wang, M.; Cui, S.; He, Y. The M-T hook structure is critical for design of HIV-1 fusion inhibitors. *J. Biol. Chem.* **2012**, *287*, 34558−34568.
(34) Liu, K.; Lu, H.; Hou, L.; Qi, Z.; Teixeira, C.; Barbault, F.; Fan, B. T.; Liu, S. W.; Jiang, S. B.; Xie, L. Design, synthesis, and biological evaluation of N-carboxyphenylpyrrole derivatives as potent HIV fusion inhibitors targeting gp41. *J. Med. Chem.* **2008**, *51*, 7843−7854.
(35) Nakata, H.; Steinberg, S. M.; Koh, Y.; Maeda, K.; Takaoka, Y.; Tamamura, H.; Fujii, N.; Mitsuya, H. Potent synergistic anti-human immunodeficiency virus (HIV) effects using combinations of the CCR5 inhibitor aplaviroc with other anti-HIV drugs. *Antimicrob. Agents Chemother.* **2008**, *52*, 2111−2119.
(36) Nagashima, K. A.; Thompson, D. A.; Rosenfield, S. I.; Maddon, P. J.; Dragic, T.; Olson, W. C. Human immunodeficiency virus type 1 entry inhibitors PRO 542 and T-20 are potently synergistic in blocking virus-cell and cell-cell fusion. *J. Infect. Dis.* **2001**, *183*, 1121−1125.
(37) Tremblay, C. L.; Kollmann, C.; Giguel, F.; Chou, T. C.; Hirsch, M. S. Strong in vitro synergy between the fusion inhibitor T-20 and the CXCR4 blocker AMD-3100. *J. Acquir. Immune. Defic. Syndr.* **2000**, *25*, 99−102.
(38) Tremblay, C. L.; Giguel, F.; Guan, Y.; Chou, T. C.; Takashima, K.; Hirsch, M. S. TAK-220, a novel small-molecule CCR5 antagonist, has favorable anti-human immunodeficiency virus interactions with other antiretrovirals in vitro. *Antimicrob. Agents Chemother.* **2005**, *49*, 3483−3485.
(39) Reeves, J. D.; Gallo, S. A.; Ahmad, N.; Miamidian, J. L.; Harvey, P. E.; Sharron, M.; Pohlmann, S.; Sfakianos, J. N.; Derdeyn, C. A.; Blumenthal, R.; Hunter, E.; Doms, R. W. Sensitivity of HIV-1 to entry inhibitors correlates with envelope/coreceptor affinity, receptor density, and fusion kinetics. *Proc. Natl. Acad. Sci. U. S. A.* **2002**, *99*, 16249−16254.
(40) Heredia, A.; Gilliam, B.; Latinovic, O.; Le, N.; Bamba, D.; Devico, A.; Melikyan, G. B.; Gallo, R. C.; Redfield, R. R. Rapamycin reduces CCR5 density levels on CD4 T cells, and this effect results in potentiation of enfuvirtide (T-20) against R5 strains of human immunodeficiency virus type 1 *in vitro*. *Antimicrob. Agents Chemother.* **2007**, *51*, 2489−2496.
(41) Francis, J. N.; Redman, J. S.; Eckert, D. M.; Kay, M. S. Design of a modular tetrameric scaffold for the synthesis of membrane-localized D-peptide inhibitors of HIV-1 entry. *Bioconjugate Chem.* **2012**, *23*, 1252−1258.
(42) Borsi, V.; Calderone, V.; Fragai, M.; Luchinat, C.; Sarti, N. Entropic contribution to the linking coefficient in fragment based drug design: a case study. *J. Med. Chem.* **2010**, *53*, 4285−4289.
(43) Ray, N. Maraviroc in the treatment of HIV infection. *Drug Des. Devel. Ther.* **2009**, *2*, 151−161.
(44) Zhao, B.; Mankowski, M. K.; Snyder, B. A.; Ptak, R. G.; Liwang, P. J. Highly potent chimeric inhibitors targeting two steps of HIV cell entry. *J. Biol. Chem.* **2011**, *286*, 28370−28381.
(45) Kopetzki, E.; Jekle, A.; Ji, C.; Rao, E.; Zhang, J.; Fischer, S.; Cammack, N.; Sankuratri, S.; Heilek, G. Closing two doors of viral entry: intramolecular combination of a coreceptor- and fusion inhibitor of HIV-1. *Virol. J.* **2008**, *5*, 56.
(46) Martinez-Munoz, L.; Barroso, R.; Dyrhaug, S. Y.; Navarro, G.; Lucas, P.; Soriano, S. F.; Vega, B.; Costas, C.; Munoz-Fernandez, M. A.; Santiago, C.; Frade, J. M. R.; Franco, R.; Mellado, M. CCR5/CD4/CXCR4 oligomerization prevents HIV-1 $gp120_{IIIB}$ binding to the cell surface. *Proc. Natl. Acad. Sci. U. S. A.* **2014**, *111*, E1960−E1969.
(47) Singer, I. I.; Scott, S.; Kawka, D. W.; Chin, J.; Daugherty, B. L.; DeMartino, J. A.; DiSalvo, J.; Gould, S. L.; Lineberger, J. E.; Malkowitz, L.; Miller, M. D.; Mitnaul, L.; Siciliano, S. J.; Staruch, M. J.; Williams, H. R.; Zweerink, H. J.; Springer, M. S. CCR5, CXCR4, and CD4 are clustered and closely apposed on microvilli of human macrophages and T cells. *J. Virol.* **2001**, *75*, 3779−3790.
(48) Chong, H.; Yao, X.; Qiu, Z.; Sun, J.; Qiao, Y.; Zhang, M.; Wang, M.; Cui, S.; He, Y. The M-T hook structure increases the potency of HIV-1 fusion inhibitor sifuvirtide and overcomes drug resistance. *J. Antimicrob. Chemother.* **2014**, *69*, 2759−2769.
(49) Su, S.; Ma, Z.; Hua, C.; Li, W.; Lu, L.; Jiang, S. Adding an artificial tail-anchor to a peptide-based HIV-1 fusion inhibitor for improvement of its potency and resistance profile. *Molecules* **2017**, *22*, 1996.
(50) Baba, M.; Miyake, H.; Wang, X.; Okamoto, M.; Takashima, K. Isolation and characterization of human immunodeficiency virus type 1 resistant to the small-molecule CCR5 antagonist TAK-652. *Antimicrob. Agents Chemother.* **2007**, *51*, 707−715.
(51) Lu, L.; Su, S.; Yang, H.; Jiang, S. Antivirals with common targets against highly pathogenic viruses. *Cell* **2021**, *184*, 1604−1620.
(52) Hoffmann, M.; Kleine-Weber, H.; Schroeder, S.; Krüger, N.; Herrler, T.; Erichsen, S.; Schiergens, T. S.; Herrler, G.; Wu, N. H.; Nitsche, A.; Müller, M. A.; Drosten, C.; Pöhlmann, S. SARS-CoV-2 cell entry depends on ACE2 and TMPRSS2 and is blocked by a clinically proven protease inhibitor. *Cell* **2020**, *181*, 271−280.e8.
(53) Tong, P.; Lu, Z.; Chen, X.; Wang, Q.; Yu, F.; Zou, P.; Yu, X.; Li, Y.; Lu, L.; Chen, Y. H.; Jiang, S. An engineered HIV-1 gp41 trimeric coiled coil with increased stability and anti-HIV-1 activity: implication for developing anti-HIV microbicides. *J. Antimicrob. Chemother.* **2013**, *68*, 2533−2544.
(54) Chou, T. C. Theoretical basis, experimental design, and computerized simulation of synergism and antagonism in drug combination studies. *Pharmacol. Rev.* **2006**, *58*, 621−681.

https://doi.org/10.1021/acs.jmedchem.1c00781
J. Med. Chem. XXXX, XXX, XXX−XXX